



Intra-center and recombination luminescence of bismuth defects in fused and unfused amorphous silica fabricated by SPCVD

Anatoly Trukhin ^{a,*}, Janis Teteris ^a, Aleksey Bazakutsa ^b, Konstantin Golant ^b

^a Institute of Solid State Physics, University of Latvia, Latvia

^b Kotel'nikov Institute of Radio-Engineering and Electronics of RAS, Russia

ARTICLE INFO

Article history:

Received 15 September 2012

Received in revised form 10 December 2012

Available online xxxx

Keywords:

Near-infrared luminescence;

UV excitation;

Bismuth doped silicon dioxide;

Luminescence decay kinetics

ABSTRACT

Photoluminescence (PL) of bismuth doped silicon dioxide excited by UV excimer lasers (ArF – 193 nm, KrF – 248 nm) and a green light laser diode (532 nm) is studied in a wide spectral band at temperatures ranging from 12 to 750 K. Two types of samples are investigated: unfused, 100 μm in thickness amorphous layer immediately deposited on the inner surface of silica substrate tube, and the same material after profusion resulted from tube collapsing to a rod by external heating. PL bands centered at 620–650 nm, 820 nm and 1400 nm wavelengths are observed in both fused and unfused samples. Under excitation by the green laser diode decay time constants for 650 nm (orange) and 1400 nm (NIR) PL bands measured at room temperature amount 3 μs and 600 μs respectively. These rather long decay times point to partly forbidden intra-center electron transitions. PL intensities of the orange and NIR bands are not temperature dependent within 12–450 K range. At higher temperatures the orange band manifests an intra-center thermal quenching, activation energy and frequency factor being 0.42 ± 0.04 eV and $5 \cdot 10^9$ s⁻¹ respectively, while intensity of the NIR band weakly depends on temperature up to 700 K. Electron-hole recombination excitation mechanism is found to contribute to the orange, but not to the NIR PL band under UV laser pumping. The specific feature of orange PL excited by recombination is the magnitude of decay time constant being about milliseconds at temperature of 12 K and decreasing with the temperature increase. Localized state ionization and two-photon absorption of intense UV light excite electron-hole pairs in silica host. Some bismuth defects serve as traps for the electrons, while holes transmute into self-trapped state thus generating self-trapped holes (STHs). Thermally activated escape of the STHs followed by their subsequent recombination with trapped electrons forms the mechanism to transfer the excitation to particular bismuth defects responsible for orange PL. At the same time no signature of the impact of such recombination process on the excitation of NIR PL is observed. This permits one to conclude that the nature of bismuth defects responsible for these two PL bands varies, and these two types of defects are available in both fused and unfused silicon dioxides.

© 2012 Elsevier B.V. All rights reserved.

1. Introduction

Bismuth-doped silica attracts more and more attention as new gain media for fiber amplifiers and lasers operating in the 1.1–1.5 μm wavelengths band [1]. Lack of alternative activators for this band distinguishes Bi doped silica fibers regardless of their currently rather poor gain properties as compared to Er- and Yb- doped fibers, which operate in longer and shorter wavelength bands.

There are two main problems to tackle. The first one is the absence of a more or less reasoned energy diagram for bismuth defect in a silica network, responsible for quantum transitions yielding lasing [2]. The second problem is the lack of immediate correlation between the increase of Bi content in silica and the increase of gain. Instead, it is observed that starting from a rather small concentration, typically not exceeding 10^{19} cm⁻³, further increase of Bi content leads to a significant decay of lasing performance of the fiber.

There are several fiber preform technologies, which have been successfully applied to fabricate Bi-doped-silica-core fibers. One of them is SPCVD – surface-plasma chemical vapor deposition [3]. Distinctive feature of this technology is the possibility to synthesize high purity and differently doped amorphous silica in the form of initially unfused material. In the process of synthesis the structure of amorphous silica is developed by immediate chemical adsorption of species from the gas phase by a substrate kept at a relatively low temperature (see [4] for more technological detail). As it was demonstrated, optical absorption and luminescence in such unfused and fused amorphous silica may be different due to the formation of additional oxygen deficient centers in the course of material fusion [5]. Gain efficiency of Bi-doped silica-core fibers drawn from the SPCVD preforms has been tested in different schemes of fiber lasers and amplifiers [6–9].

The results of recent experiments on near-infrared (NIR) photoluminescence (PL) pumped by 808 and 980 nm wavelength laser diodes in fused and unfused SPCVD silica speak for weakly bonded to the glass host bismuth interstitial species rather than strongly chemically incorporated in the SiO₂ network ions as a

* Corresponding author. Tel.: +371 7260 686; fax: +371 7132778.

E-mail address: truhins@cfi.lu.lv (A. Trukhin).

tentative model for the defects responsible for NIR PL [10]. Current study is aimed at searching more information regarding luminescence of Bi-associated defects in fused and unfused silica fabricated by SPCVD using different types of material excitation by high-energy photons. Particular attention is paid to temperature dependences of luminescence parameters (decay time and intensity) which for the case of Bi-related defects in silica have not been studied in detail yet. Comparison study of as deposited unfused Bi doped silica film and its fused counterpart reflects possible impact of the fiber fabrication process on NIR luminescence.

2. Sample synthesis and luminescence measurements

As it is mentioned above amorphous material immediately deposited in the SPCVD is unfused. Its structure is formed on the inner surface of a silica substrate tube at a rather low (1000–1200 °C) temperature. In our experiments Heraeus F300 silica tubes 20 mm in outer diameter and 2 mm wall thickness are used as substrates. In order to trace possible effect of fusion on luminescence we fabricated two deposited one by one layers of about 100 μm in thickness each. Bi-doped silicon dioxide (the first layer) is covered by undoped silica (the second layer) to prevent bismuth escape during subsequent tube collapsing by external heating. Vapors of anhydrous BiCl_3 together with other halides mixed with oxygen and nitrous oxide are used as a starting gas mixture supplied to the reaction zone of the scanning plasma column. After deposition the tube is collapsed into a preform only on half the deposited length (~15 cm). The other half of the tube with the deposited on its inner surface amorphous material remains uncollapsed, and is used as unfused sample for luminescence measurements. According to X-ray microanalysis bismuth concentration in the samples is as high as 10^{18} cm^{-3} .

Fig. 1 illustrates refractive index profile of the collapsed part of the tube. It is seen that bismuth contributes to an increase of silica's refractive index. Oscillations in the refractive index profile are associated with intentional variations of BiCl_3 flow during the deposition. Refractive index profile of the collapsed part of the tube sample was measured with the help of York Technology P102 refractive index preform analyzer.

The as-deposited unfused film sample is colored in yellow-orange. After the tube collapsing Bi-doped region in the form of a ring is also colored in yellow-orange, while bismuth free center of the preform (see Fig. 1) remains uncolored. Fused and unfused samples are cut from collapsed and uncollapsed parts of the tube perpendicular to

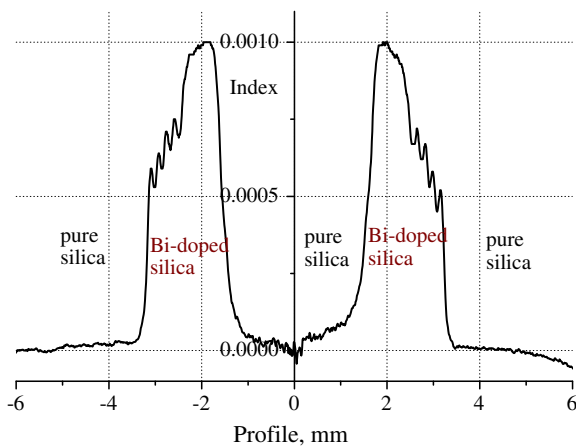


Fig. 1. Refractive index profile of collapsed Bi-doped two-layer silica structure. Ripples in the outer layer demonstrate a possibility to manage bismuth content in the glass by means of BiCl_3 evaporation temperature control in the SPCVD technology (see ref. [3] for more technological detail).

its axis. Two opposite sides of both samples are optically polished. Both samples provide visually observable orange luminescence under different excitations.

ArF (193 nm) and KrF (248 nm) model PSX-100 excimer lasers of Neweks, Estonia (pulse energy ~5 mJ, pulse duration ~5 ns, beam cross-section $\sim 2 \times 2 \text{ mm}$), as well as green (532 nm) pulsed diode laser of CryLas, Germany (~1 ns pulse duration) are used for luminescence excitation. PL is recorded by means of a MDR-3 grating monochromator equipped by photomultiplying tubes (PMTs) H6780-04 for UV-vis (200–800 nm) and H10330A-45 for NIR (900–1400 nm) spectral bands as photoreceivers. Both PMTs are loaded with 50 Ω resistors. Luminescence decay curves averaged by 128 runs are registered with the help of Tektronic TDS 2022B oscilloscope. Time-resolved PL spectra are obtained from recorded decay curves (for each wavelength) integrated within time interval partitioned into nanosecond and millisecond sub-bands. The errors of measurements estimated from a scatter of several registration runs typically do not exceed 5–10%. For the cases of small signals, the influence of PM noise and stray currents of excitation sources is marginally larger, which is reflected via corresponding error bars in the figures.

Time-average PL spectra are also traced under the same pulsed lasers excitation with the help of two other different spectrometers. The Hamamatsu model C10082CAH and Ocean Optics model NIR-512 mini-spectrometers for 200–800 nm and 1000–1700 nm wavelength bands respectively are used for this purpose.

PL measurements are performed at 11–650 K sample temperatures. For measurements at temperatures 11–300 K cooling by a helium refrigerator is applied. For measurements at higher temperature a resistor was used as a heater. The samples are carefully cleaned and mounted on a holder, no glue is used. PL light is collected in a direction perpendicular to the exciting laser beam.

3. Results

3.1. Intra-center excited luminescence

The main PL bands, which can be excited in the samples under investigation, are presented in Fig. 2. Four bands can be stood out: NIR bands at ~1400 nm and 820 nm, an orange band at 620–650 nm and a UV band at 300 nm. UV band is observed only under ArF laser excitation in the fused sample.

Temperature dependences of decay time constant and time-resolved intensity of the orange PL excited by the 532 nm laser are

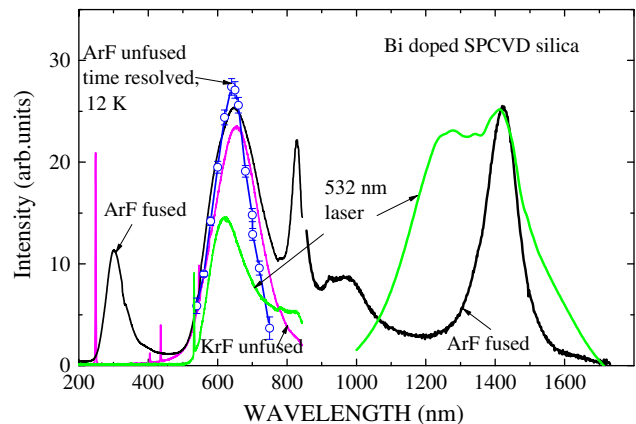


Fig. 2. Time-average photoluminescence spectra of Bi doped SPCVD silica measured at 293 K with the help of Hamamatsu in the range of 200–800 nm and Ocean Optics NIR 512 in the range of 1000–1700 nm minispectrometers. Scatter plot (circles) corresponds to spectrum built up by means of integrating the decay curves recorded at 12 K at each particular wavelength. The spectra are not normalized by the instrument function. Types of samples and pulsed lasers used for PL pumping are indicated inside the plot. The NIR band under 532 nm laser is smoothed.

presented in Fig. 3. It is seen that neither decay time constant nor intensity depends on temperature within experimental errors in the range of 60–450 K. At temperatures above 450 K process of thermal quenching takes place with a relatively good correspondence between thermal behavior of intensity (I) and decay time constant (τ). Both dependencies can be well fitted by Mott expressions for thermal quenching in crystals [11]: $I(T) = I_0(1 + f \cdot \tau_0 \exp(-E_a/kT))^{-1}$, $\tau = \tau_0(1 + f \cdot \tau_0 \exp(-E_a/kT))^{-1}$, where I_0 is the intensity of non-quenched transitions, τ_0 – independent on temperature decay time constant, f – frequency factor, E_a – activation energy, T – temperature, and k – Boltzmann constant. The above approximation gives 0.42 ± 0.04 eV for the activation energy with frequency factor of about $5 \cdot 10^9 \text{ s}^{-1}$. Insertion in Fig. 3 shows well exponential behavior for the 650 nm luminescence decay that is is not quite typical for disordered materials. On the other hand in disordered materials thermal quenching manifests itself as an exponential growth of luminescence intensity with cooling. The fact that the measured thermal quenching obeys the Mott law typical for crystalline materials could mean that the center responsible for orange luminescence is well isolated from silica network. Orange luminescence kinetics excited by ArF and/or KrF lasers in addition to the 3 μs decay time component contains a slower term. Time constant of this slower component increases with the decrease of temperature (Fig. 5).

In the case of ArF laser excitation orange luminescence intensity linearly depends on excitation intensity which testifies to one photon excitation process. In the case of KrF laser excitation dependence of PL intensity on pump one obeys characteristic for two-photon process power law (Fig. 5).

3.2. Luminescence excited in recombination process

Under ArF laser excitation the slower component of orange PL decay corresponds to 1–2 ms time interval at temperature of 11 K (Fig. 4). Both unfused and fused samples demonstrate similar kinetics. Temperature dependences of time resolved luminescence intensity and decay time constant are presented in Fig. 6. Heating of samples leads to a decrease of decay time constant from 1 to 2 ms at 11 K to $\sim 20 \mu\text{s}$ at 100 K whereas the intensity calculated by the integration of decay curves grows up with heating. At temperatures exceeding 100 K the intensity drops down, but with much smaller rate as compared to the decay time constant decrease. This result is similar for both fused and unfused samples and to the first approximation it does not depend on material preparation conditions. Important is the fact that the decrease of intensity correlates with thermally activated escape of self-trapped holes, which is illustrated in Fig. 6 by a curve taken from ref. [16,12].

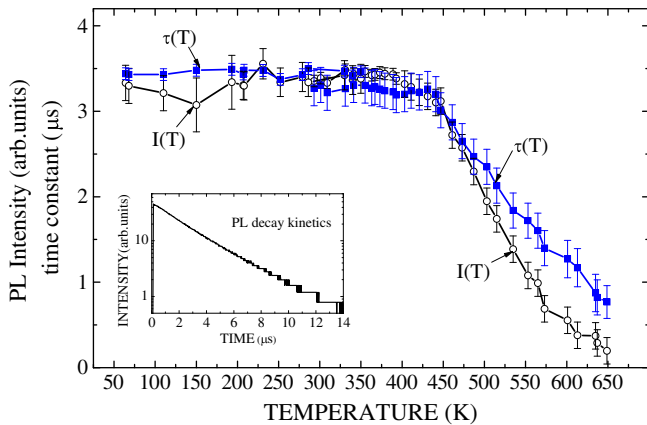


Fig. 3. Intensity and decay time constant (see inset) of the orange (650 nm wavelength) luminescence band excited by 532 nm wavelength pulses as a function of temperature. Activation energy of thermal quenching amounts to 0.42 ± 0.04 eV, frequency factor being $5 \cdot 10^9 \text{ s}^{-1}$.

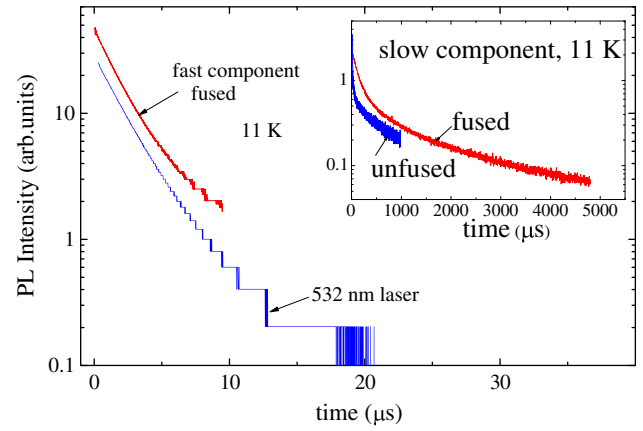


Fig. 4. Decay kinetics of orange (650 nm wavelength) photoluminescence pumped by ArF (193 nm wavelength), and green (532 nm wavelength, decay is similar in the range 80–400 K) laser pulses. Inset plot displays decay kinetics of a slow component observed under the ArF laser pump.

Insufficient sensitivity of all our photoreceivers in the vicinity of 800 nm wavelength did not allow us to get much information regarding peculiarities of the 820 nm luminescence band. Fig. 7 illustrates that parameters of this PL band excited by the ArF laser pulses (time resolved spectra and decay time constant) do not depend on temperature in the range of 12–293 K. Luminescence decay time at 820 nm is larger than that of the band at 650 nm and is about 10–15 μs . No slow component is detected for the 820 nm band.

The UV band at 300 nm is also non-exponential (Fig. 8) and its decay kinetics becomes faster with temperature increase (Fig. 8, inset). It is significant that acceleration of decay process with heating occurs faster than corresponding decrease of luminescence intensity calculated by the integration of corresponding decay curves. So, the band at 300 nm behaves similar to the band at 650 nm excited by the ArF laser.

3.3. NIR luminescence

NIR PL at 1400 nm exhibits practically exponential decay with time constant of about 650 μs (Fig. 9). NIR luminescence intensity at 1400 nm weakly depends on temperature ranging from 11 K to 700 K. We cannot measure decay kinetics in the whole above range of temperatures, but decay kinetics is temperature independent in 11 K–300 K interval within experimental errors. There are some peculiarities in the decay curves. Some signal growth in the beginning

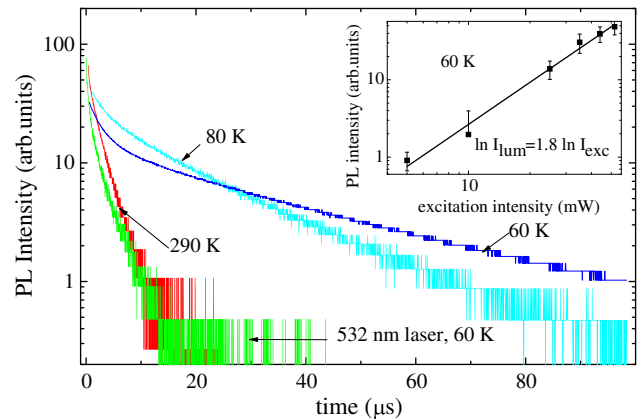


Fig. 5. Decay kinetics of orange (650 nm wavelength) photoluminescence pumped by the KrF (248 nm wavelength) laser in unfused Bi-doped SPCVD silica at different temperatures. Inset shows dependence of PL intensity on pump power. Kinetics decay under 532 nm laser is presented for comparison.

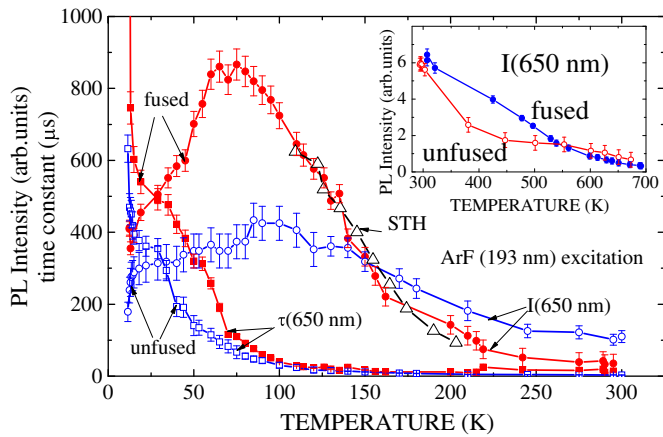


Fig. 6. Temperature dependencies of time resolved luminescence intensity and decay time constant excited by the ArF laser 650 nm wavelength PL intensity determined as an integral under recorded decay curves (circles) and effective decay time constant (close squares). Note non-exponential character of the decay and its strong dependence on temperature. Time average orange PL intensity as a function of elevated temperatures measured with the help of Hamamatsu minispectrometer is depicted in the inset. Temperature dependence of the ESR signal correspondent to the self-trapped hole (STH) center in silica glass taken from [16] is plotted for comparison.

of the decay process as well as some bending of the decay curves can be seen, which likely could be caused by an overload of the PMT. In Fig. 10 we present decay curves for NIR PL measured at a shorter wavelength (~1000 nm). It is seen that decay kinetics is different for fused and unfused samples and also differs from that of the 1400 nm band.

4. Discussion

4.1. The origin of 300 nm luminescence band

One can highlight several PL bands excited by UV and green lasers, which correlate with the presence of bismuth in amorphous silicon dioxide. First is the PL band centered at 300 nm. The band can be excited by 193 nm wavelength laser and is observed in fused sample only. This band appears to be not immediately associated with electron transitions between steady state energy levels of a Bi related defect, but is rather combined with an oxygen deficient center. The latter is known to be formed in SPCVD silica due to profusion [5].

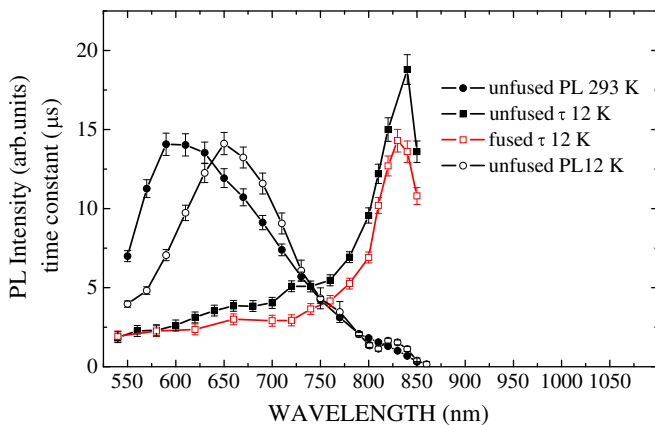


Fig. 7. Silica glass (SPCVD) with Bi PL and τ spectra under ArF laser pulses. Properties of the 820 nm wavelength luminescence band in comparison with the orange one recorded by time resolved regime for fused and unfused samples measured at 293 K and 12 K. The band at 820 nm possesses decay time constant about 10–15 μ s higher than that of orange luminescence excited in intra center process. Intensity and decay time constant of 820 nm band are independent on temperature in the range 12–293 K.

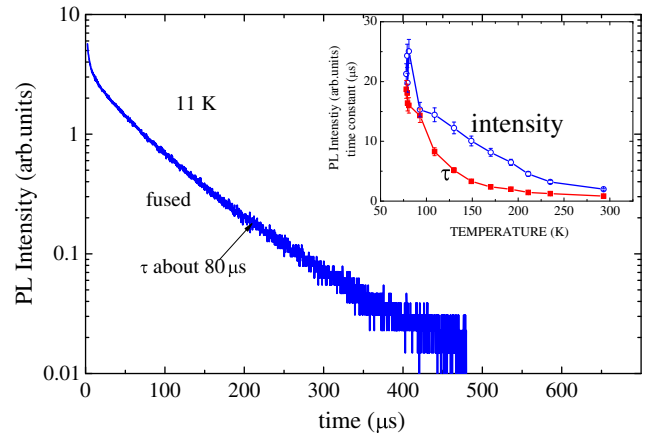


Fig. 8. Decay kinetics of 300 nm wavelength PL band pumped by the ArF laser in fused SPCVD silica sample with Bi. Temperature dependencies of decay time constant and intensity determined by the integration of decay curves are shown in the inset.

4.2. Possible model for 650 nm luminescence center

Next is the orange band centered at wavelength of 650 nm. Being excited via an intra-center process by means of the 532 nm wavelength laser, PL of this band decays with time constant (τ_0) of about 3.5 μ s, which is temperature independent up to 400 K (Fig. 3). We can attribute this band to partly forbidden transitions owing to a relatively slow decay. For allowed transition time constants lay in a nanosecond range of time. Temperature dependences of the decay time constant as well as the luminescence intensity at higher temperatures indicate that thermal quenching starts to occur only at temperatures exceeding 450 K, activation energy and frequency factor being 0.42 ± 0.04 eV and $5 \cdot 10^9$ s $^{-1}$ respectively. This shows that the green laser excitation yields mainly intra-center luminescence.

Let us consider possible models for orange luminescence. First of all we exclude Bi $^{3+}$ ions because we did not observe phenomena specific to triplet–singlet luminescence of $^3P_1-^1S_0$, i.e. strong dependence on temperature transition probabilities [13,14]. Next candidates could be Bi $^{2+}$ ($6s^26p^1$) or Bi $^+$ ($6s^26p^2$) with p–p transitions, which are forbidden according to the Laporte rule. If Laporte rule is applicable to the center responsible for orange luminescence excited via an intra-center process and independent on temperature in a wide range prior to thermal quenching, a static group of symmetries for the defect responsible for such kind of PL should not contain a center of inversion. The defect is some kind of an asymmetrical irregularity, which contains bismuth incorporated in its structure.

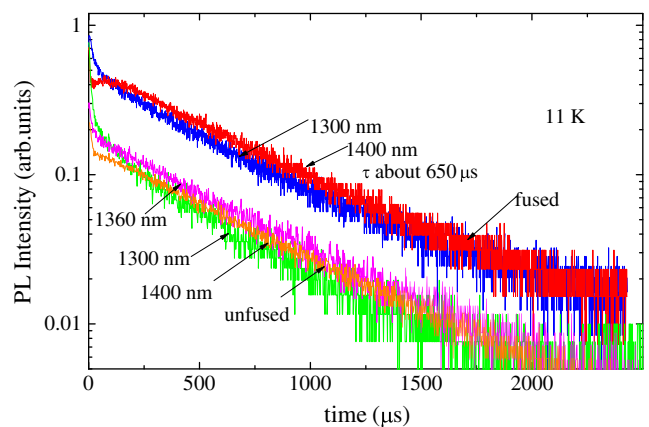


Fig. 9. Decay kinetics of NIR luminescence pumped by the ArF laser measured at different wavelengths with the help of the H10330A-45 PM at temperature of 11 K in fused and unfused Bi doped silica samples fabricated by SPCVD.

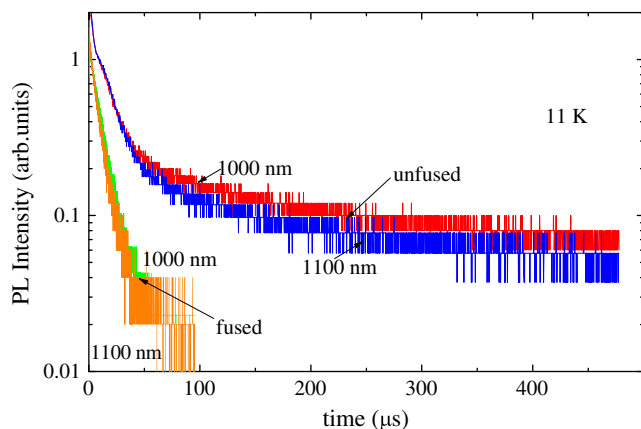


Fig. 10. Decay kinetics of NIR PL under the ArF laser pumping measured at wavelengths in the vicinity of 1000 nm with the help of H10330A-45 PM at temperature of 11 K in fused and unfused Bi doped silica samples fabricated by SPCVD.

We have no enough motivation for a particular decision between Bi^{2+} or Bi^+ point defects or even some clusters of bismuth proposed in [15], as a model for such irregularity. Main reason is that the center should be an electron trap, which then could recombine with a hole.

4.3. Participation of 650 nm luminescence center in recombination processes

In the case of UV (ArF laser) excitation an additional slow component contributes to the decay of the orange PL band, decay time constant being as high as several ms at temperature of 11 K. Increase of this decay time constant with cooling is accompanied by decrease of luminescence intensity (Fig. 5). Such behavior indicates that a recombination process is involved in the luminescence excitation. At a lower temperature trapping of charges prevails, thus preventing them from recombination. With temperature increase above 100 K intensity of UV excited orange PL decreases together with decrease of decay time constant. However, intensity decreases slower than decay time constant does. That could be explained by a thermal release of the trapped separated charges, which starts to contribute to orange PL intensity via the excitation of bismuth defects through recombination having no impact on the decay time constant.

Character of the decrease of UV excited orange PL intensity with temperature increase (Fig. 5) well coincides with that one characteristic for the ESR signal associated with STHs [12]. This enables one to suppose that they are the STHs, which escape under the temperature increase, move to Bi related recombination centers containing trapped electrons. STHs could partly disappear via nonradiative processes thus diminishing their contribution to luminescence excitation through the recombination. Relatively short recombination life time adduced over fast decay kinetics (Fig. 5) could indicate that the recombination takes place presumably between closely situated pairs of an electron and a self-trapped hole formed under the ArF laser excitation. The recombination of such pairs likely comprises a thermally stimulated process. Cooling down to 11 K leads to the decrease of luminescence intensity accompanied by a huge increase of the decay time constant.

According to [16] the orange PL band at 650 nm in bismuth containing silicate glasses is attributed to Bi^{2+} ions. Although reference [16] contains no evidence for this statement, this model could be supported by following reasoning. Demonstrated in our experiment probable participation of STHs in the recombination processes associated with the excitation of orange PL band implies the availability of electrons located on stable traps. Bi^{2+} is a good candidate for such trap. If it is, the center with a trapped electron should look like Bi^+ . Actually we could not exclude that the center of luminescence for 650 nm band can be associated with Bi^+ as well. If so the center with a trapped electron should be Bi^0 .

4.4. Processes of NIR luminescence excitation

The NIR band centered at wavelength of 1400 nm is the most important one for lasing. According to [10] the energy diagram for bismuth defects yielding this kind of PL could be thought as a three level system, in which transitions from an upper level to the ground state correspond to PL band centered at 820 nm, whereas the ones from an intermediate metastable state produce 1400 nm wavelength NIR PL.

Neither intensity nor decay kinetics depend on temperature for the 1400 nm NIR PL band excited by high energy photons. Significant is that in our experiments with high energy photons excitation we did not find any signature of the impact of recombination process mentioned above on either 820 nm or 1400 nm PL bands. This means that these defects do not participate in trapping of electrons excited in host by intense UV light. Low probability of charge trapping serves as additional argument in favor of interstitial nature of defects responsible for NIR PL in fused and unfused SPCVD silica. It is also clear that PL bands centered at 650 nm and 1400 nm wavelengths belong to bismuth defects of very different nature, simultaneously coexisting in silica host.

Important question regarding a structural model for bismuth interstitials responsible for NIR PL in silica remains open. A pair of bismuth atoms or ions as well as BiO molecule could serve as candidates for the model [15,17]. We failed, however, to find an ESR signal from the SPCVD Bi doped silica film cooled down to 77 K. This means that the interstitials are ESR silent or the temperature was too high.

5. Conclusion

Two types of fundamentally different luminescence defects associated with the presence of bismuth in free of other additives fused and unfused amorphous silica fabricated by SPCVD are revealed. The first one can be excited via both intra-center photon absorption and electron-hole recombination processes. These defects are characterized by the orange luminescence band centered at 620–650 nm wavelength with decay time constant of about 3 μs . At temperatures greater than 450 K this PL band is exposed to an intra-center thermal quenching with activation energy of 0.42 ± 0.04 eV and frequency factor of about $5 \cdot 10^9$ s^{-1} . Defects of this type can serve as electron traps for separated electron-hole pairs excited in the host through two-photon absorption of intense UV laser light. Recombination of these trapped electrons with holes provides a channel for the excitation of orange PL characterized by specific temperature dependences of intensity and decay kinetics.

The second type of bismuth defect is responsible for the NIR luminescence band centered at 1400 nm. This band does not manifest thermal quenching up to the temperature of 700 K. By contrast to the orange band, we did not find evidence in favor of any contribution of the recombination process mentioned above to the excitation of NIR PL.

Lack of the excitation via recombination process as well as very different temperature dependences of intensities and decay time constants observed for the orange and NIR PL bands testify to different nature of corresponding types of bismuth defects. If for the orange PL band subvalent bismuth chemically incorporated in the silica network could be such a defect, the NIR PL band is likely associated with bismuth interstitials occupying voids of the network and thus cannot trap free electrons excited by UV and traveling in the conductivity band of the SiO_2 host.

Acknowledgments

This work is supported by the Latvian Council grant as well as the Material Science program (IMIS). The spectral-kinetics investigations are supported with ERAF project 2010/0275/2DP//2.1.1.1.0/10/APIA/VIAA/124.

References

- [1] Y. Fujimoto, M. Nakatsuka, *Jpn. J. Appl. Phys.* 40 (2001) L279; E.M. Dianov, *Optical Fiber Communication Conference (OFC) OSA Technical Digest* (Optical Society of America, 2012), paper OW4D.1, 2012.
- [2] Evgeny M. Dianov, *J. Non-Cryst. Solids* 355 (2009) 1861–1864.
- [3] K.M. Golant, A.P. Bazakutsa, O.V. Butov, Yu.K. Chamorovskij, A.V. Lanin, S.A. Nikitov, *The 36th European Conference and Exhibition on Optical Communication, ECOC 2010, Torino, Italy, 2010*, p. 1.
- [4] K.M. Golant, *Defects in SiO₂ and related dielectrics: science and technology*, in: G. Pacchioni, L. Skuja, D.L. Griscom (Eds.), *NATO Science Series II: Mathematical and Physical Chemistry*, vol. 2, Kluwer, 2000, p. 427.
- [5] A.N. Trukhin, K.M. Golant, J. Teteris, *J. Non-Cryst. Solids* 358 (2012) 1538–1544.
- [6] E.J.R. Kelleher, J.C. Travers, Z. Sun, A.C. Ferrari, K.M. Golant, S.V. Popov, *J.R. Taylor, Laser Phys. Lett.* 7 (2010) 790.
- [7] B.H. Chapman, E.J.R. Kelleher, K.M. Golant, S.V. Popov, *J.R. Taylor, Opt. Lett.* 36 (2011) 1446.
- [8] Ben H. Chapman, Edmund J.R. Kelleher, Sergei V. Popov, Konstantin M. Golant, Janne Puustinen, Oleg Okhotnikov, James R. Taylor, *Opt. Lett.* 36 (2011) 3792.
- [9] A. Chamorovskiy, J. Rautiainen, A. Rantamäki, K.M. Golant, O.G. Okhotnikov, *Opt. Express* 19 (2011) 6433.
- [10] A.P. Bazakutsa, O.V. Butov, E.A. Savel'ev, K.M. Golant, *J. Commun. Technol. Electron.* 57 (2012) 743.
- [11] D. Curie, *Luminescence in Crystals*, Wiley, New York, 1963, p. 194.
- [12] D.L. Griscom, *J. Non-Cryst. Solids* 149 (1992) 137.
- [13] S.G. Zazubovich, V.V. Khizniakov, *Izv. Akad. Nauk SSSR, Ser. Fiz.* 49 (1985) 1874.
- [14] A. Trukhin, *J. Non-Cryst. Solids* 123 (1990) 250.
- [15] A.N. Romanov, Z.T. Fattakhova, A.A. Veber, O.V. Usovich, E.V. Haula, V.N. Korchak, V.B. Tsvetkov, L.A. Trusov, P.E. Kazin, V.B. Sulimov, *Opt. Express* 20 (2012) 7212.
- [16] J. Ren, J. Qiu, D. Chen, X. Hu, X. Jiang, C. Zhu, *J. Alloys Compd.* 463 (2008) L5.
- [17] M. Peng, J. Qiu, D. Chen, X. Meng, C. Zhu, *Opt. Lett.* 30 (2005) 2433.